

Supporting Information

Time-Dependent Density Functional Theory for X-Ray Absorption Spectra: Comparing the Real-Time Approach to Linear Response

John M. Herbert,^{1,2*} Ying Zhu,^{1,2} Bushra Alam,¹ and Avik Kumar Ojha¹

¹*Department of Chemistry & Biochemistry,
The Ohio State University, Columbus, Ohio, 43210 USA*

²*Chemical Physics Graduate Program,
The Ohio State University, Columbus, Ohio, 43210 USA*

August 26, 2023

*herbert@chemistry.ohio-state.edu

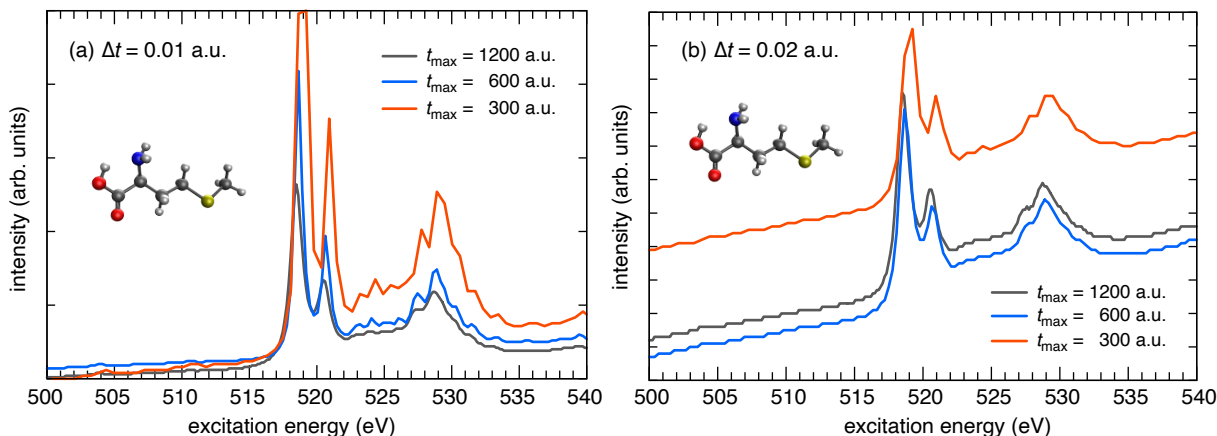


Figure S1: TDKS spectra near the oxygen K-edge for methionine, computed at the B3LYP/6-31G(d) level for different simulation times t_{\max} , with a time step of (a) $\Delta t = 0.01$ a.u. versus (b) $\Delta t = 0.02$ a.u.. These spectra were computed using a conventional FFT, without the use of Padé approximants. Spectra for $t_{\max} = 1200$ a.u. are the same as those in Fig. 1.

Molecule	Functional	Excitation	Excitation Energy (eV)					
			Expt. ^a	6-311(2+,2+)G**	6-311(+,+)G**	cc-PVTZ	aug-cc-PVTZ	def2-TZVPD
H ₂ CO	SRC1-r1	O(1s) → π*	530.82	530.92	530.92	530.98	531.04	530.96
	SRC2-r1	O(1s) → π*	530.82	530.82	530.82	530.90	530.94	530.84
	SRC1-r1	C(1s) → π*	285.59	285.62	285.62	285.67	285.63	285.57
(CH ₃) ₂ CO	SRC1-r1	O(1s) → π*	531.3	531.35	531.35	531.40	531.46	531.38
	SRC2-r1	O(1s) → π*	531.3	531.08	531.08	531.14	531.18	531.09
	SRC1-r1	C(1s) → π*	287.10	286.07	286.06	286.13	286.08	286.02
Uracil	SRC1-r1	O(1s) → π*	532.10	531.78	531.78	531.85	531.89	531.81
Methionine	SRC1-r1	O(1s) → π*	532.44	532.28	531.27	532.38	532.40	532.32

^aData from Refs. 1–5. ^bMean absolute deviation, with respect to experiment.

Table S1: Comparison of the performance of various basis sets for LR-TDDFT, as applied to oxygen and carbon K-edge excitations for small molecules.

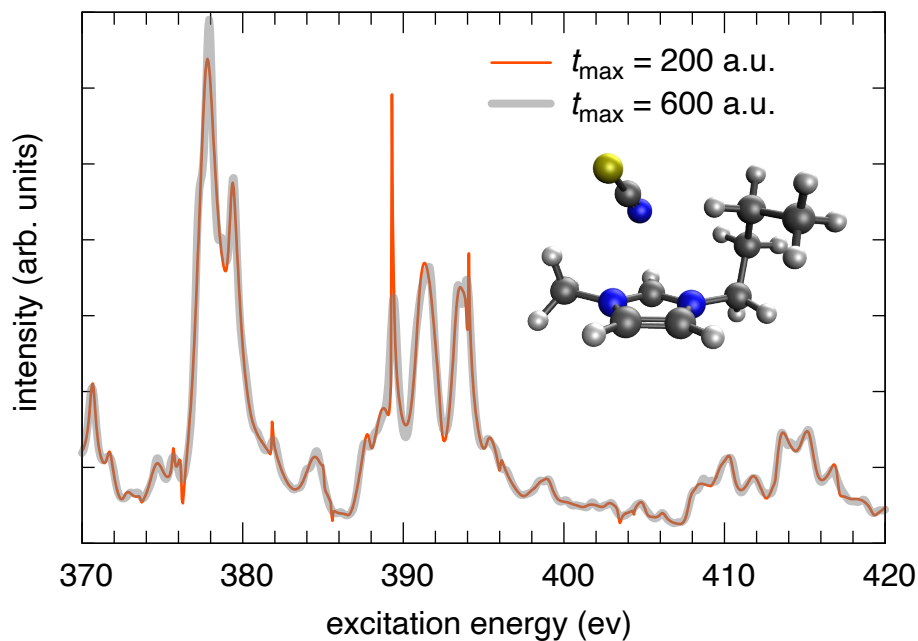


Figure S2: TDKS spectra near the nitrogen K-edge for the ionic liquid dimer $[\text{C}_4\text{C}_1\text{Im}^+][\text{SCN}^-]$, computed at the B3LYP/6-311(2+,2+)G(d,p) level. The spectrum for $t_{\text{max}} = 600$ a.u. is the same as that shown in Fig. 6, and is compared where to a simulation based on 1/3 of the propagation time, using Padé approximants in both cases. Minor artifacts are evident in the latter spectrum.

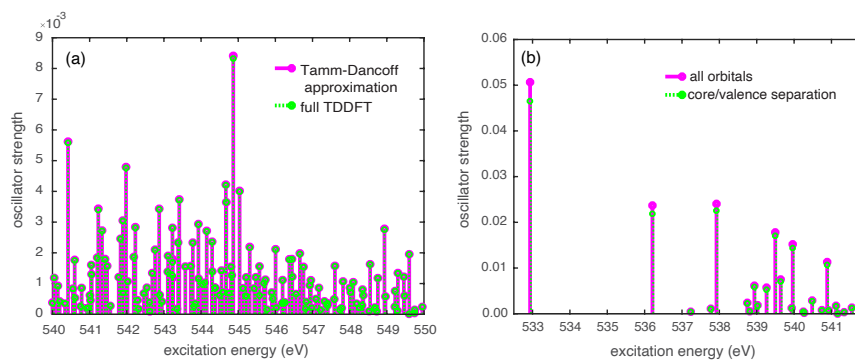


Figure S3: LR-TDDFT convergence tests for methionine spectra at the oxygen K-edge. (a) Test of the Tamm-Dancoff approximation (in which y is neglected) versus a full LR-TDDFT calculation, performed at the SRC1-r1/def2-TZVPD level. (b) Test of the CVS approximation at the SRC1-r1/6-31G(d) level, comparing to a calculation in which all orbitals are active.

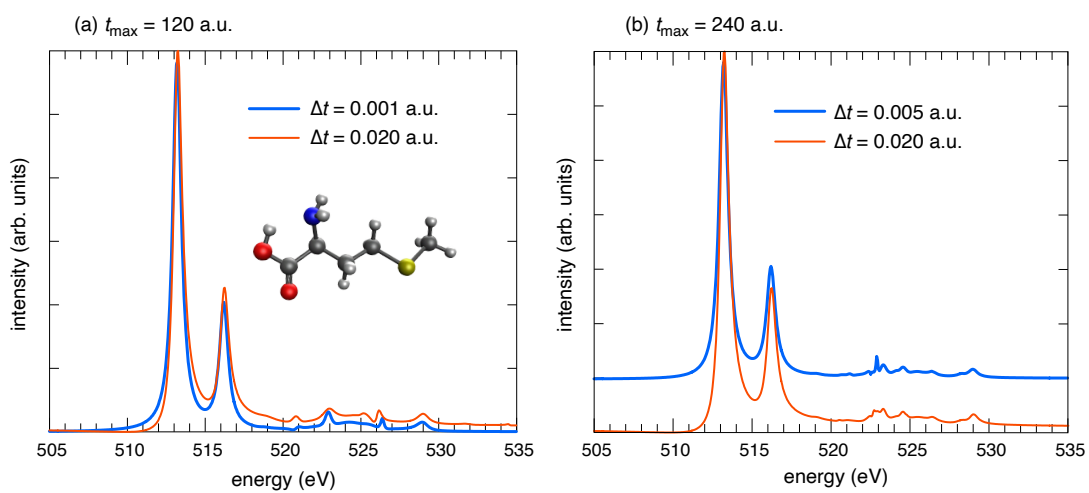


Figure S4: TDKS simulations of XAS for methionine at the oxygen K-edge, computed at the B3LYP/STO-3G level with different time steps, for total propagation times of (a) $t_{\max} = 120$ a.u. (≈ 2.9 fs), versus (b) $t_{\max} = 240$ a.u. (≈ 5.8 fs). All spectra were computed using Padé approximants.

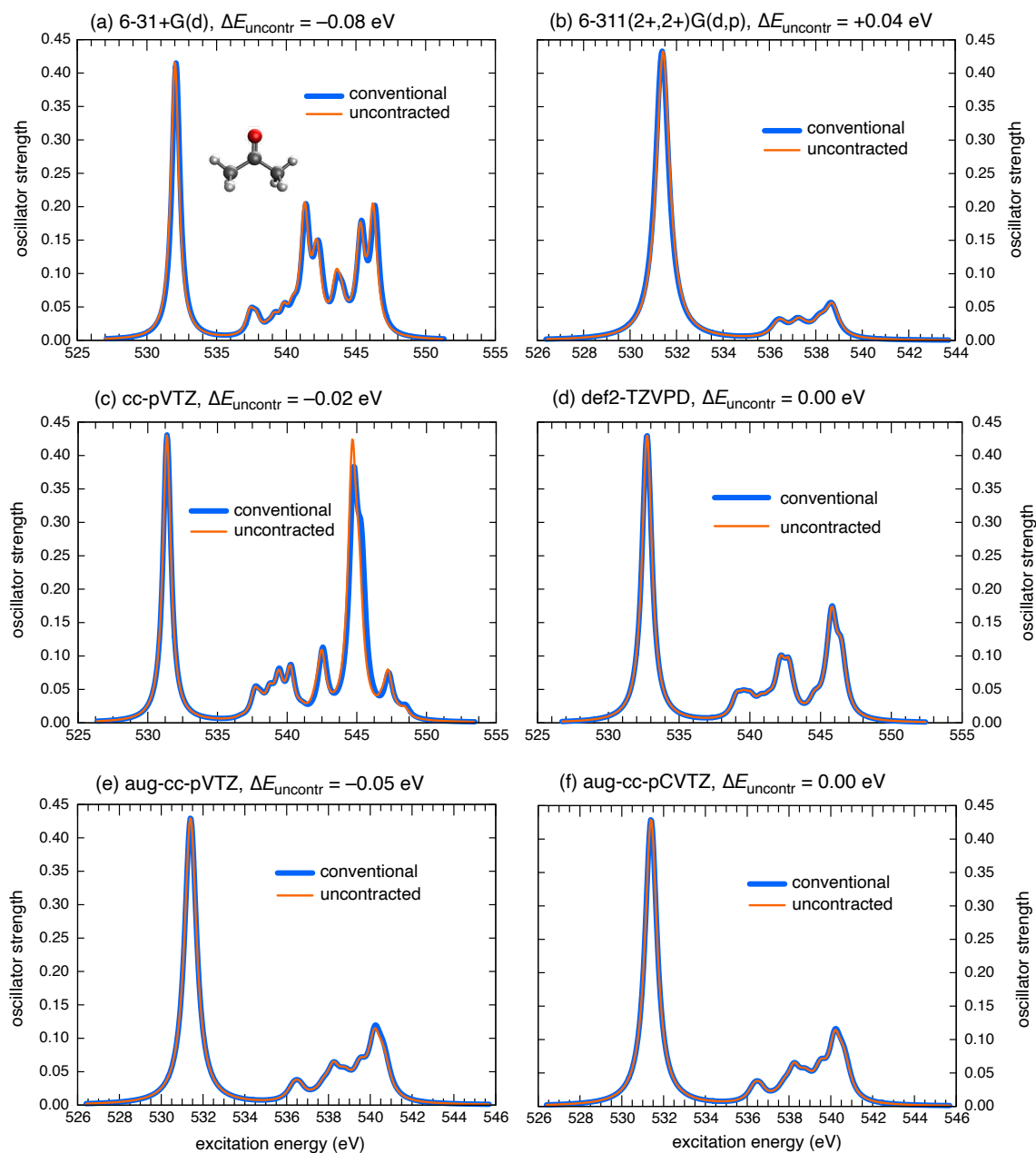


Figure S5: LR-TDDFT/CVS spectra of acetone at the oxygen K-edge using various basis sets. All spectra include the lowest 25 excited states, within the O(1s) CVS approximation, and have been broadened using a Lorentzian function with a width of 0.7 eV, consistent with other LR-TDDFT results presented in this work. In each case, results are present for the conventional basis set alongside a version in which the core functions have been uncontracted. The quantity $\Delta E_{\text{uncontr}}$ is the energy shift in the O(1s) \rightarrow LUMO transition upon uncontracting the basis set.

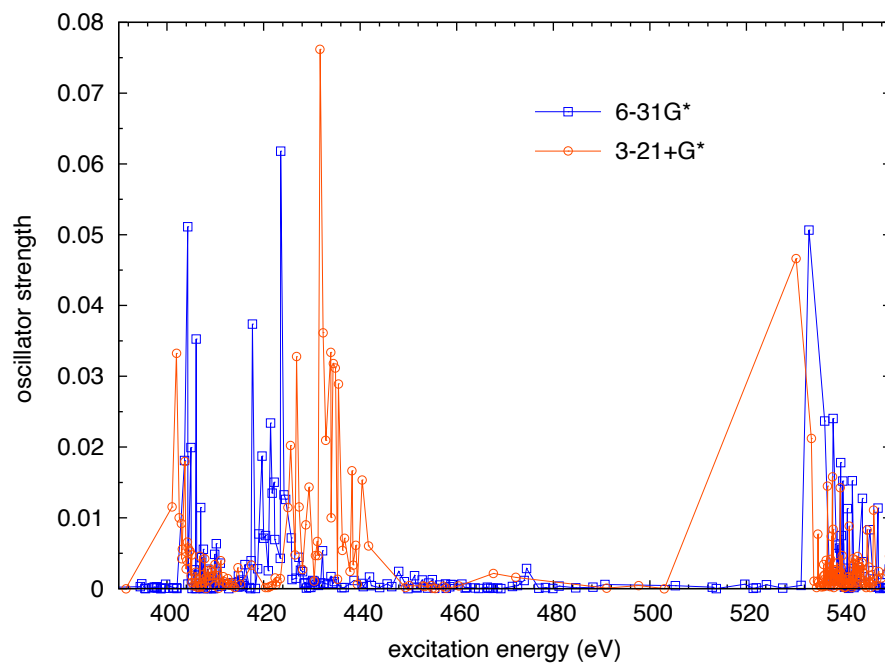


Figure S6: LR-TDDFT spectrum of methionine, computed using the SRC1-r1 functional in two different basis sets, by computing all $o \times v$ roots of the \mathbf{A} matrix in Eq. (22). (What is plotted is excitation energy versus oscillator strength for the sequence of states, and the lines that connect the data points are a guide for the eye rather than a properly broadened intensity profile.) The section of the spectrum that is shown here connects the nitrogen K-edge (starting just above 400 eV) with the oxygen K-edge starting around 530 eV. It can be seen that there is a semi-continuous sequence of spectroscopically dark excitations that connect the two, corresponding to excitations from N(1s) to very high-energy virtual orbitals that constitute orthogonalized discretized continuum states. Looking at the spectrum just below 400 eV, it is clear that C(1s) \rightarrow continuum excitations are present right up to the nitrogen K-edge.

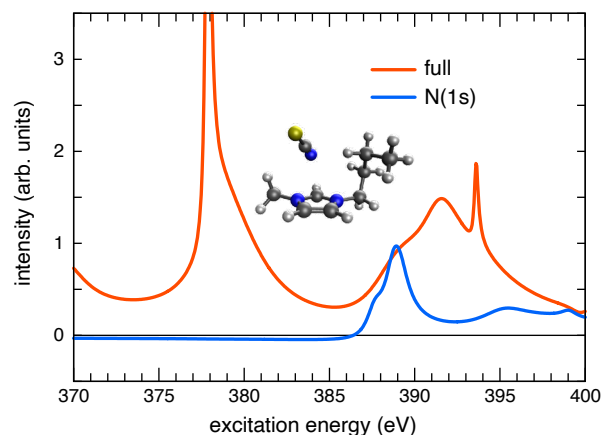


Figure S7: TDKS spectra near the nitrogen K-edge for the ionic liquid dimer $[\text{C}_4\text{C}_1\text{Im}^+][\text{SCN}^-]$, computed at the B3LYP/6-311(2+,2+)G(d,p) level using $t_{\text{max}} = 37.5$ a.u. of simulation time, *i.e.*, only half as long as the simulation in Fig. 7a. The too-short simulation time causes the two near-edge peaks in the filtered N(1s) spectrum to merge.

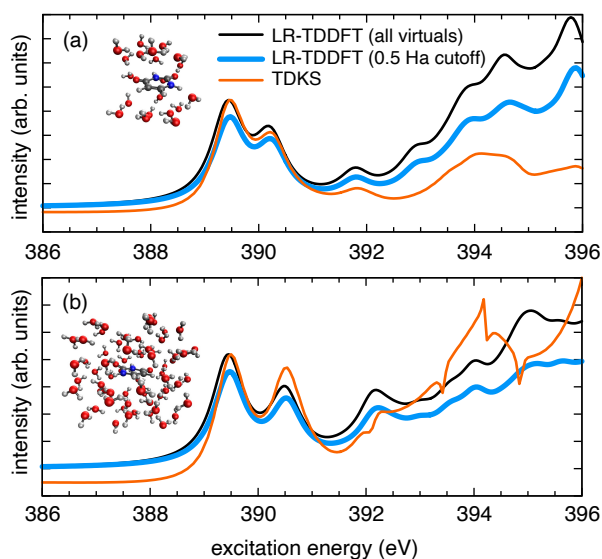


Figure S8: TDDFT spectra near the nitrogen K-edge for (a) $(\text{uracil})(\text{H}_2\text{O})_{21}$ and (b) $(\text{uracil})(\text{H}_2\text{O})_{68}$, computed at the CAM-B3LYP/6-31G(d) level. The TDKS spectrum (in orange) and the LR-TDDFT/CVS spectrum (in black) are the same as those in Fig. 9, computed using $\Delta t = 0.02$ a.u. and $n = 100$ states, respectively. The thicker blue curve shows a LR-TDDFT/CVS spectrum that is also computed using 100 states but with a virtual orbital cutoff of $0.5 E_h$. Both LR-TDDFT spectra are plotted on the same absolute scale (oscillator strength), whereas the TDKS spectrum has been scaled to match the intensity of the first peak in the LR-TDDFT spectrum with no cutoff.

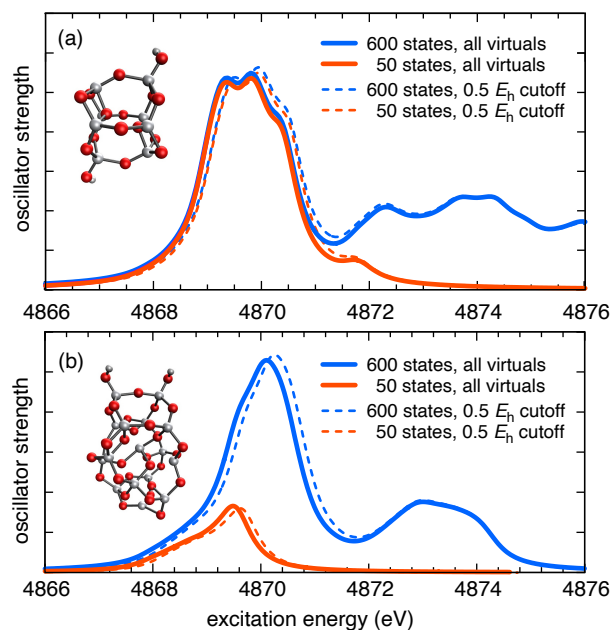


Figure S9: LR-TDDFT/CVS spectra at the titanium K-edge for (a) $\text{Ti}_8\text{O}_{16}\text{H}_2$ and (b) $\text{Ti}_{16}\text{O}_{32}\text{H}_2$, computed at the PBE0/def2-SV(P) level. Spectra including all virtual orbitals in the active space are the same as those plotted in Fig. 10, whereas the dashed spectra include only those virtual MOs with $\varepsilon_a < 0.5 E_h$. The absolute scale is absolute oscillator strength.

References

- [1] Sham, T. K.; Yang, B. X.; Kirz, J.; Tse, J. S. K-edge near-edge x-ray-absorption fine structure of oxygen-and carbon-containing molecules in the gas phase. *Phys. Rev. A* **1989**, *40*, 652–669.
- [2] Hitchcock, A. P.; Brion, C. E. Inner-shell excitation of formaldehyde, acetaldehyde and acetone studied by electron impact. *J. Electron Spectrosc.* **1980**, *19*, 231–250.
- [3] Remmers, G.; Domke, M.; Puschmann, A.; Mandel, T.; Xue, C.; Kaindl, G.; Hudson, E.; Shirley, D. A. High-resolution *K*-shell photoabsorption in formaldehyde. *Phys. Rev. A* **1992**, *46*, 3935–3944.
- [4] Zubavichus, Y.; Shaporenko, A.; Grunze, M.; Zharnikov, M. Innershell absorption spectroscopy of amino acids at all relevant absorption edges. *J. Phys. Chem. A* **2005**, *109*, 6998–7000.
- [5] Fujii, K.; Akamatsu, K.; Muramatsu, Y.; Yokoya, A. X-ray absorption near edge structure of DNA bases around oxygen and nitrogen K-edge. *Nucl. Instrum. Meth. B* **2003**, *199*, 249–254.